Nucleic Acids Research, 1998, Vol. 26, No. 23 **5409–5416**

Optimization of excimer-forming two-probe nucleic acid hybridization method with pyrene as a fluorophore

Masayuki Masuko*, Hiroyuki Ohtani[1], Katsuyoshi Ebata[1,+] and Akira Shimadzu[1]

Tsukuba Research Laboratory, Hamamatsu Photonics K. K., Tokodai, Tsukuba 300-2635, Japan and
[1]Department of Biomolecular Engineering, Faculty of Bioscience and Biotechnology, Tokyo Institute of Technology, Nagatsuta, Midori-ku, Yokohama 226-0026, Japan

Received August 7, 1998; Revised and Accepted October 14, 1998

ABSTRACT

A previously presented homogeneous assay method, named the excimer-forming two-probe nucleic acid hybridization (ETPH) method, is based on specific excimer formation between two pyrenes attached at the neighboring terminals of two sequential probe oligonucleotides complementary to a single target. In this study, we investigated assay conditions and optimal molecular design of probes for intense excimer emission using a pyrenemethyliodoacetamide-introduced 16mer probe, a pyrene butanoic acid-introduced 16mer probe and a target 32mer. The length of the linker between the pyrene residue and the terminal sugar moiety remarkably influenced the quantum efficiency of excimer emission; the pair of linker arms of these two probes was optimal. The quantum efficiency was also dependent upon the concentrations of dimethylformamide and NaCl added to the assay solution. Spectroscopic measurements and T_m analysis showed that an optimal configuration of the two pyrene residues for intense excimer emission might be affected by pyrene–pyrene interaction, pyrene–duplex interaction (intercalation/stacking) and solvent conditions as a whole. We then demonstrated the practicality of the ETPH method with the optimal hybridization conditions thus attained by determining that the concentration of 16S rRNA in extracts from *Vibrio mimicus* ATCC 33655 cells in exponential growth phase is 18 500 16S rRNA molecules/cell on average.

INTRODUCTION

An excimer, usually seen in quenching processes of aromatic hydrocarbons in condensed phase, is a complex between a molecule in the excited state (^{1}M*) and the same species in the ground state (^{1}M), namely ^{1}M* + ^{1}M ↔ (^{1}M*.^{1}M) ↔ ^{1}D* (1). It is characterized by its fluorescence spectrum; a broad band shifted to longer wavelengths with respect to the structured monomer emission band. The formation of excimers of aromatic hydrocarbons is restricted to a parallel, cofacial configuration with an interplanar distance of 3–4 Å (1–3). These unique characteristics enabled researchers to develop various application methods for biophysical and polymer analyses; e.g. probing the dynamics of membranes *in vitro* and *in vivo* (4), observing enzyme–substrate and protein–protein reactions (5,6), interpreting the conformational change of polymers and proteins (7,8), and detecting guest molecules by the host–guest interaction of cyclodextrins (9). All these applications use excimer emission with a large Stokes shift for the real-time observation of a specific chemical reaction or of the dynamic changes in physical parameters of materials.

Nucleic acid hybridization is the formation of sequence-specific, base-paired duplexes from any combination of nucleic acid fragments. Since its first description by Schildkraut *et al*. (10), hybridization methods have been essential techniques for >35 years, not only for advancing our understanding of gene structure and function, but also for diagnosing illnesses, for criminal identification in forensic investigations, etc. (11). The majority of hybridization methods use oligonucleotide probes artificially labeled with markers, such as radioisotopes, fluorescent dye molecules, enzymes and biotin (12). However, a common disadvantage is that the excess probe which must be added to the hybridization solutions must be removed using solid surfaces, such as gels, microtiter plates and membrane filters (13). Consequently, the methods are tedious and time-consuming. To overcome these disadvantages, several homogeneous hybridization assay methods have been proposed (14,15). To our knowledge, however, other than the PCR monitoring method based on fluorescence resonance energy transfer (16), these methods are not yet satisfactory for practical use in laboratories.

This lack of a practical method is the reason we developed a novel hybridization method called the excimer-forming two-probe hybridization (ETPH) method (17; Fig. 1), which uses two different oligonucleotide probes for hybridization. The sequences of these probes run sequentially on the complementary target. Neighboring terminals, one in the 3′-position of one probe and the other in the 5′-position of the other probe, are each labeled with one excimer-forming fluorophore. Upon hybridization, these fluorophores come into close proximity and form an excimer. The excimer fluorescence with characteristically large Stokes shift can be easily discriminated from the monomer fluorescence,

*To whom correspondence should be addressed. Tel: +81 298 47 5161; Fax: +81 298 47 5266; Email: masuko@hpk.trc-net.co.jp

+Present address: Chemicals Research Laboratories, LION Corporation, 13-12 Hirai 7-chome, Edogawa-ku, Tokyo 132-0035, Japan

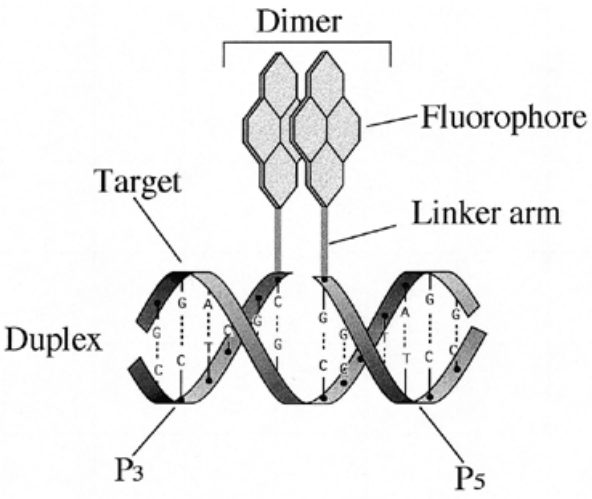

Figure 1. Principle of the ETPH method, where the fluorophores can come into close proximity upon hybridization between the two probes and the target.

thereby allowing homogeneous hybridization assays to be done even in the presence of excess unhybridized probes. In a previous study (17) using pyrene as a model fluorophore, we demonstrated that hybridization actually induces the formation of an excimer. Moreover, Mann *et al*. (18) pointed out that the introduction of lipophilic moieties, such as pyrene, into oligonucleotides may lead to increased transport of the nucleotides across cell membranes, resulting in easy staining of target nucleic acids. If this is true, the ETPH method holds promise as an *in vivo* technique for real-time imaging of target nucleic acids, because it requires no washing of excess probes out of a cell.

In this study, we clarified assay solution conditions and determined an optimal molecular design of probes for intense excimer emission using pyrene-labeled probes having linker arms of different length between a sugar moiety and a pyrene residue. Clarifying the assay solution is important for laboratory use of the ETPH method and determining the optimal probe design is important for extending the method to aromatic hydrocarbons other than pyrene. Because the 1-pyrenebutyric acid hydrazide-introduced probe that we used in a previous study (17) is thermochemically unstable (19), in this study we mainly used a 1-pyrenebutanoic acid-introduced probe. Using the probes and assay conditions thus attained, we then demonstrated that the ETPH method could be applied to homogeneous assays by using it to detect *Vibrio mimicus* 16S rRNA.

MATERIALS AND METHODS

Target and probe oligonucleotides

The model target (hereafter denoted Tar) for detection was a 32mer deoxyribonucleotide with the same sequence as described previously (17). This sequence is part of the 16S rRNAs of *V.mimicus* and *Vibrio cholerae* (when T residues are replaced by U residues). The central portion (position 11–27) of Tar is a sequence to specify species of *V.cholerae* and *V.mimicus* (position 1260–1276 in their rRNAs) (20). This region is suitable for the detection of these bacteria in their natural habitat (21).

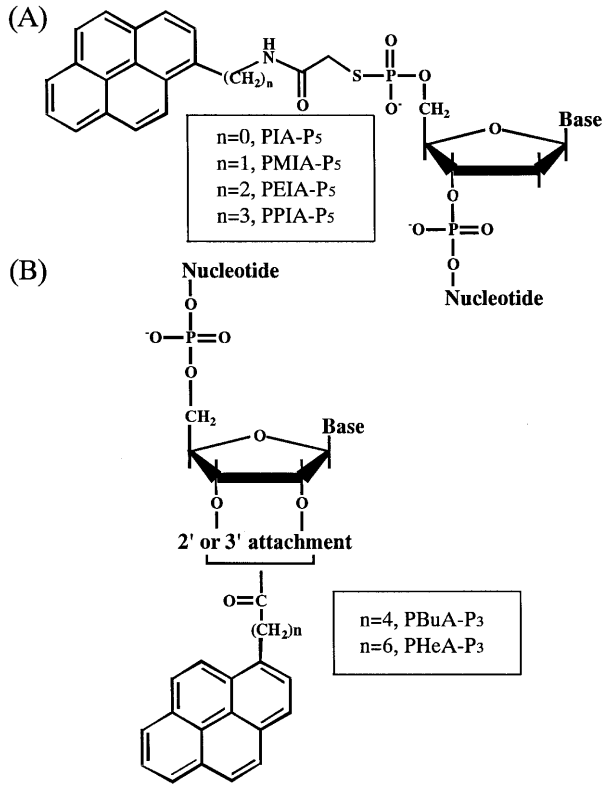

Figure 2. Terminal structures of the pyrene-labeled hybridization probes. (**A**) The 5′-terminal of P_5 (PXIA-P_5) and (**B**) the 3′-terminal of P_3 (PYA-P_3).

Probes for the detection of Tar were two different 16mer deoxyribonucleotides that run sequentially and that are complementary to the Tar 32mer; 3′-TCTCCCGTGCCTATGG-5′ and 3′-[C]GCTCCACCTCGCTTA-5′ (designated P_5 and P_3, respectively), where [C] designates the ribonucleotide that is the only exception. Calculated using an empirical equation (22), the predicted free energy changes in the hybridization reactions between the probes and their corresponding target sequences were similar (–32.5 and –34.2 kcal/mol for P_5 and P_3, respectively; 1 M Na^+ in the absence of formamide at pH 7.0 and 25°C). Furthermore, the possibility of hairpin–stem formation was negligible. All the nucleotides were purchased from Rikaken, Japan.

Introduction of pyrene residues into the probes

A pyrene residue was attached to the 5′-OH of the 5′-terminal deoxyribose of P_5 (Fig. 2A) by the method of Czworkowski *et al*. (23) using *N*-(1-pyrene)iodoacetamide (PIA), *N*-(1-pyrenemethyl)-iodoacetamide (PMIA), *N*-(1-pyreneethyl)iodoacetamide (PEIA) and *N*-(1-pyrenepropyl)iodoacetamide (PPIA) as precursor dye molecules that had different lengths of methylene chains, $[-CH_2-]_n$ (n = 0, 1, 2 or 3). [These precursors (Molecular Probes, USA) are designated PXIAs, and the probes PMIA-P_5 and PXIA-P_5s.] We purified these probes using HPLC with an octadecylsilyl silica gel column (17). After condensation with an evaporator centrifuge and ethanol precipitation, the preparations were dissolved in 0.1 M phosphate buffer (pH 7.0) and stored at –80°C until use.

A pyrene residue was attached to the 3′-terminal ribose of P_3 (Fig. 2B) by the carbonyldiimidazole (CDI) method (24) using 1-pyrenebutanoic acid (PBuA) and 1-pyrenehexanoic acid (PHeA) as precursors (Molecular Probes). (Generally, the precursors are designated PYAs, and the probes PBuA-P_3 and PYA-P_3s.) The preparations were purified to remove unreacted oligonucleotides and precursor dyes by HPLC using the same conditions used for PXIA-P_5 (17). The fraction with the initial simultaneous appearance of an absorbance peak at 260 nm and a fluorescence peak at 375 nm (excitation at 345 nm) was collected. Further treatments were the same as those described in the preceding paragraph for PXIA-P_5s. The product may be present as a mixture of 2′-OH- and 3′-OH-labeled isomers (25). We used this isomer mixture without further separation.

Determination of the concentrations of target, probe oligonucleotides, PXIA-P_5s and PYA-P_3s

The concentrations of target and unlabeled probe oligonucleotides were determined from the absorbances at 260 nm (A_{260}) in 0.1 M phosphate buffer (pH 7.0), based on their calculated extinction coefficients (26): Tar, 326.4; P_5, 139.9; P_3, 136.4/mM/cm. The concentration of the pyrene-labeled probe was also obtained from the A_{260} of its oligonucleotide portion. However, the A_{260} of the pyrene-labeled probe was the overlap of the A_{260} values of its pyrene moiety and the oligonucleotide portion. We therefore estimated the contribution of the pyrene moiety to the total A_{260} by assuming that the A_{260}:$A_{peak\ (\sim 345)}$ ratios of the spectra of the corresponding PXIAs and PYAs in the standard hybridization solution (*loc. cit.*) were the same as those of the spectra of labeled oligonucleotides in 0.1 M phosphate buffer (pH 7.0): PIA, 0.45; PMIA, 0.29; PEIA, 0.34; PPIA, 0.31; PBuA, 0.26; PHeA, 0.27. Thus, we calculated the A_{260} of the oligonucleotide portion using the following equation

$$\begin{aligned} A_{260}^{\text{Oligo}} &= A_{260}^{\text{Pyr-oligo}} - A_{260}^{\text{Pyr}} \\ &= A_{260}^{\text{Pyr-oligo}} - A_{260}^{\text{Pyr-oligo}} \times A_{260}^{\text{PXIA or PYA}} / \\ &\quad A_{\text{peak}\ (\sim 345)}^{\text{PXIA or PYA}} \end{aligned} \quad \mathbf{1}$$

Hybridization

The standard hybridization solution used for this study contained 10 mM phosphate buffer (pH 7.0), 20% (v/v) dimethylformamide (DMF) and 0.2 M NaCl. In many cases, we added 100 nM each of PMIA-P_5, PBuA-P_3 and Tar to this solution. After this mixture was allowed to set for at least 10 min, spectroscopic measurements were done at 25°C (standard hybridization conditions) unless otherwise stated.

Determination of fluorescence quantum efficiency

Fluorescence quantum efficiency (ϕ_{samp}) was obtained by comparing the integrated fluorescence spectra of a sample (F_{samp}) with that of a standard sample (F_{std}) that has a known fluorescence quantum efficiency (ϕ_{std}) (27)

$$\phi_{samp} = \phi_{std} \times (K_{std}/K_{samp}) \times (n_{samp}/n_{std})^2 \times (F_{samp}/F_{std}) \quad \mathbf{2}$$
$$[F = \int f_{\bar{\nu}}\, d\nu = \int f_{\bar{\lambda}}\, \lambda^2\, d\lambda]$$

where K represents absorbance at the wavelength of excitation, n is refraction index and $f_{\bar{\nu}}$ and $f_{\bar{\lambda}}$ denote wave number-scaled and wavelength-scaled fluorescence spectra, respectively. We used quinine sulfate dissolved in 0.5 M sulfuric acid (ϕ_{std} = 0.546; 28) as a standard.

Melting curve and melting temperature (T_m)

The melting curve of each hybrid was obtained by determining the A_{270} of the solution as a function of temperature. It took ~20 min for the solution to reach temperature equilibrium after each 5°C incremental increase. The solution in the cuvette was stirred with a magnetic stirrer and the temperature was measured with a platinum resistance thermoprobe (Model R003; Chino, Japan) inserted into the cuvette through a sealed cap. The 100% level of dissociation (i.e. complete dissociation) in the melting curve was defined as an absorbance change of <0.5%/3°C change. In our experiments, 0 and 100% occurred at 25 and 65°C, respectively. For the apparent melting curves, we used the profiles of fluorescence intensity versus temperature determined using the procedures described above for the absorbance measurements.

Instrumentation

Absorbance measurements were done using a UV-2500 (PC) S spectrophotometer (Shimadzu, Japan) with a cuvette whose light path length was 1.0 cm. Excitation and emission spectra were measured using a 850 spectrofluorometer (Hitachi, Japan) with a 1-cm square cuvette. The spectrofluorometer was calibrated using a rhodamine B-based quantum counter and a scatterer. In all of the spectra data, the background emission from the buffer alone was subtracted. The circular dichroism (CD) spectra were recorded using a J-600 CD spectrometer (JASCO, Japan).

Determination of 16S rRNA of *V.mimicus*

We used the 16S rRNA of *V.mimicus* ATCC 33655 as a model target for the ETPH method. Several loopfuls of the precultured bacteria were inoculated into 100 ml of a broth containing peptone and NaCl (29) in a 500 ml Erlenmeyer flask and then aerobically cultivated with a shaker at 30°C. Eighty milliliters of the culture in exponential growth phase were harvested by centrifugation and the resulting pellet of bacteria was lysed to extract RNA with TRI Reagent® (Molecular Research Center, USA) according to the manufacturer's instructions. The resulting pellet of RNA was then dissolved in H_2O. In parallel with this procedure, cells in a unit volume of the culture were counted by an ordinary plating method using a solid medium of Vibrio Agar Nissui® (Nissui Pharmaceutical, Japan).

The concentration of 16S rRNA in an extract was determined under the standard hybridization conditions by the ETPH method except for two differences: the standard hybridization solution also contained 2 mM EDTA, and the hybridization mixtures were incubated initially at 55°C for 10 min and then successively at 25°C for >50 min.

Reagents and experimental conditions

The DMF used for PXIA-P_5 syntheses and hybridization assays was dehydrated by refluxing with CaH_2 after pre-dehydration with molecular sieves. T4 polynucleotide kinase was purchased from Takara Shuzo (Japan) and adenosine-5′-*O*-(3-thiotriphosphate) used for PXIA-P_5 synthesis, from Boeringer Mannheim (Germany). The reagents prepared were either filtered with a filtration unit (Sterifil®-D; Millipore, USA) or autoclaved. All the experimental procedures were done in a clean booth (Class 100) except when

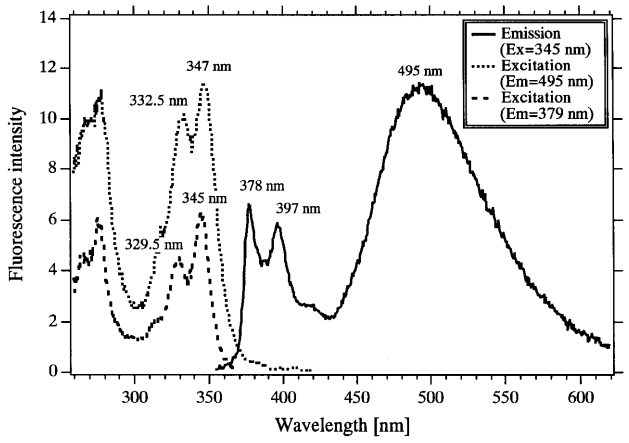

Figure 3. Excitation and emission spectra of the hybrid between PMIA-P_5/PBuA-P_3 and Tar at 25°C. The sample was the standard hybridization solution (Materials and Methods) containing 100 nM each of these nucleotides.

capped vessels and cuvettes were used. When RNA was manipulated, all the vessels and cuvettes were sterilized to inactivate RNase according to the established methods (30).

RESULTS AND DISCUSSION

Excitation and emission spectra of the hybrid between PMIA-P_5/PBuA-P_3 and Tar

A broad emission band with a maximum at 495 nm was observed (Fig. 3) in addition to structured monomer emission bands below 450 nm. Evidence that this 495 nm band is attributable to pyrene excimer emission includes these three characteristics of excimers: (i) the shape and position of the band was similar to those of pyrene excimer emissions previously reported (1,31); (ii) the intensities of the monomer bands and the 495 nm band weakened and intensified, respectively, with increasing concentration of the target added to the hybridization solution (1,17,31); (iii) the excitation spectra recorded at 379 (monomer) and 495 nm (excimer) were almost the same (Fig. 3).

Absorption and emission spectra of the pyrene-introduced probes

To help interpret pyrene excimer formation, we looked at the spectral characteristics of pyrene-labeled probes and their hybrids not accompanied by excimer formation. A comparison of the absorption spectrum for PBuA-P_3 and that for its precursor PBuA shows that the maximum (346 nm) in the UV spectrum of PBuA-P_3 was red-shifted by 2 nm relative to that (344 nm) of PBuA dissolved in the standard hybridization solution (data not shown). A similar tendency was also recognized for PHeA-P_3 and for PIA-, PMIA-, PEIA- and PPIA-P_5s. Using the extinction coefficients of oligonucleotide portions at 260 nm (Materials and Methods), we determined the extinction coefficients of pyrene residues in PMIA-P_5 and PBuA-P_3 at 350 nm to be 25.8 and 22.7/mM/cm, respectively, in 0.1 M phosphate buffer (pH 7.0).

A comparison of the emission spectra for PBuA-P_3 and PBuA indicates that pyrene monomer emission was remarkably quenched (91%) by the introduction of a pyrene residue into P_3 (data not shown). Such quenching also occurred for PMIA-P_5 (81% quenching). The degree of such quenching is more significant in the absence than presence of DMF, and depends on the nucleotide sequence and the presence of pyrimidine nucleotides (32,33). The monomer emissions of both PBuA-P_3 and PMIA-P_5 were further quenched upon hybridization when one of the probes was not labeled with a pyrene residue (i.e. hybrids between PBuA-P_3/P_5 and Tar, and between P_3/PMIA-P_5 and Tar). The fluorescence quantum efficiencies of the precursor dye molecules show the pyrene monomer emission to be quenched by 95 and 83% in the PBuA-P_3 and PMIA-P_5 duplex formations, respectively.

There was no difference in absorption spectra of the pyrene-labeled probes (PBuA-P_3 and PMIA-P_5) before and after hybridization with Tar.

Effect of DMF concentration on excimer emission intensity

From a practical viewpoint, the addition of formamide to a hybridization buffer is effective for weakening the base pairing of duplexes so that an adequate T_m value can be chosen for hybridization stringency (34,35). Furthermore, a water-soluble organic solvent may influence the fluorescence quantum efficiency of pyrene through pyrene–solvent dipole–dipole interactions (36). We therefore added DMF, which has an effect similar to that of formamide, to a hybridization solution for intense pyrene excimer emission. The maximum intensity of excimer emission occurred at a DMF concentration between 30 and 40% (Fig. 4A) and decreased as the concentration was increased further. In contrast, due to dissociation of the duplex into single strands, monomer emission increased sharply when the DMF concentration exceeded 40%. One of the standard hybridization conditions was set at a DMF concentration of 20% because the fraction of excimer fluorescence (at 495 nm) to monomer fluorescence (at 378 nm) was maximal around this concentration. The effects of DMF concentration on other pyrene monomer emissions (the mixture of PMIA-P_5 and PBuA-P_3, the hybrid between PMIA-P_5 and Tar) are shown in Figure 4B.

Effect of NaCl concentration on excimer formation

Monovalent cations, such as Na^+, influence the equilibrium constant and the rate of duplex formation because they dissipate the negative charge of phosphate (37–39). Generally, as the Na^+ concentration increases to 0.2 M, the equilibrium shifts toward duplex formation and the formation rate increases. Furthermore, NaCl affects the interactions (e.g. intercalation) between nucleic acid chains and non-ionic aromatic hydrocarbons, such as pyrene and benzo[*a*]pyrene. This effect depends on whether or not these molecules are conjugated to the chains through covalent linkages (18,40,41). The higher the concentration of Na^+, the stronger the interactions become when the chains are single-stranded, and the weaker when double-stranded (18). We therefore examined these NaCl effects on the pyrene excimer formation that accompanies hybridization. NaCl remarkably influenced the intensity of excimer fluorescence: the intensity increased until it peaked at an NaCl concentration of 0.1 M, after which it reached a plateau (data not shown). The rate of excimer formation was also affected: in the absence of NaCl, the rate was extremely low, whereas in the presence of 0.2 M NaCl, the excimer intensity reached hybridization equilibrium in 10 min. These effects on the intensity coincide with those reported previously (38,39). Our results show that NaCl exerts its effect indirectly on excimer formation through its effect on duplex formation. Furthermore,

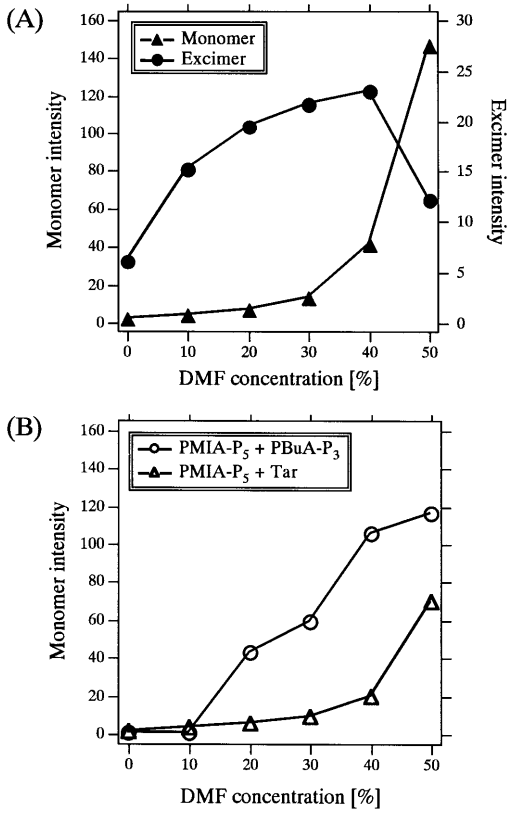

Figure 4. Effect of DMF on hybrid formation (**A**) between PMIA-P_5/PBuA-P_3 and Tar and (**B**) between PMIA-P_5 and Tar without PBuA-P_3. Also shown in (B) is the effect on dye-labeled probes without Tar. The effects were evaluated at 25°C by measuring fluorescence intensities at 495 nm (for excimer) and 378 nm (for monomer) with 345 nm excitation. The concentration of each dye-labeled probe and Tar was 100 nM except for the hybrid between PMIA-P_5 and Tar (200 nM each). The solvent was the standard hybridization solution (Materials and Methods).

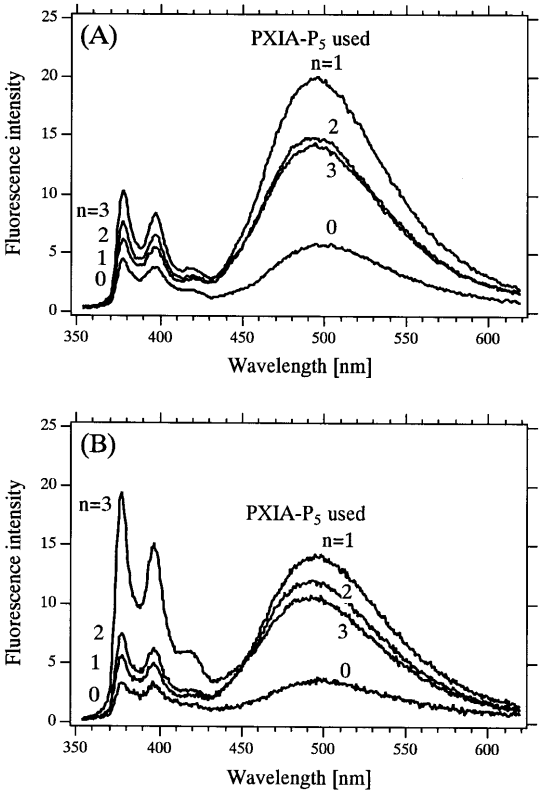

Figure 5. Effect of length of the linker arm between the terminal sugar moiety and the pyrene residue (Fig. 2) on excimer formation. Excimer formation was evaluated at 25°C by measuring emission spectra with 345 nm excitation. (**A**) Hybridization between PBuA-P_3 (n = 4)/PXIA-P_5 (n = 0–3) and Tar. (**B**) Hybridization between PHeA-P_3 (n = 6)/PXIA-P_5 (n = 0–3) and Tar. The concentration of each dye-labeled probe and Tar was 100 nM. The solvent was the standard hybridization solution (Materials and Methods).

these results also show that addition of 0.2 M NaCl is necessary for the standard hybridization conditions and that spectroscopic measurements should be taken a minimum of 10 min after initiation of duplex formation.

Effect of length of the linker arms between the pyrene residue and the sugar moiety of the probes on excimer formation

Excimer formation of aromatic hydrocarbons is initiated by collision between excited and unexcited molecules, i.e. is a diffusion-controlled reaction in solution (1,3,31). Furthermore, the relative configuration between the molecules strongly affects excimer formation (1), especially in crystals (2,42) and intramolecular dimers (43). We previously showed that the intensity of pyrene excimer emission significantly decreases when the two probes are further separated by inserting one or two extra nucleotides into the central portion of the target where the terminals of the complementary probes meet (17). This means that for efficient excimer formation, separation between neighboring terminals of the probes should be a few angstroms; nevertheless, the pyrenes are conjugated to sugar moieties with to some extent flexible linker arms.

For further characterization of the ETPH method and its future application to fluorophores other than pyrene, it is crucial to find the optimal combination of linker arms of the probes. We therefore prepared four types of PXIA-P_5 and two types of PYA-P_3 and then combined them to obtain fluorescence spectra. The length of linker arms strongly influenced the intensity of pyrene excimer emission (Fig. 5). From a comparison of PXIA-P_5s with the common probe PBuA-P_3, the intensity of pyrene exicimer emission in decreasing order was PMIA-P_5 > PEIA-P_5 > PPIA-P_5 > PIA-P_5 (Fig. 5A). The order was the same when PHeA-P_3 replaced PBuA-P_3 as the common probe (Fig. 5B). Emission was more intense for PBuA-P_3 than for PHeA-P_3. Although PYA is a mixture of 2′-OH- and 3′-OH-labeled isomers, the orders for PXIAs and PYAs were the same for all preparations of PYA used in this study. Because these results show that the optimal set of probes was the PMIA-P_5/PBuA-P_3 system, we used this probe combination for other experiments unless otherwise mentioned.

Melting curves for the duplexes

In general, both intercalation of aromatic hydrocarbons, such as pyrene, into a duplex and stacking onto a base quench the fluorescence of these hydrocarbons (18,44). We therefore evaluated the strength of these interactions for intense excimer emission in the ETPH method. Because such interactions can

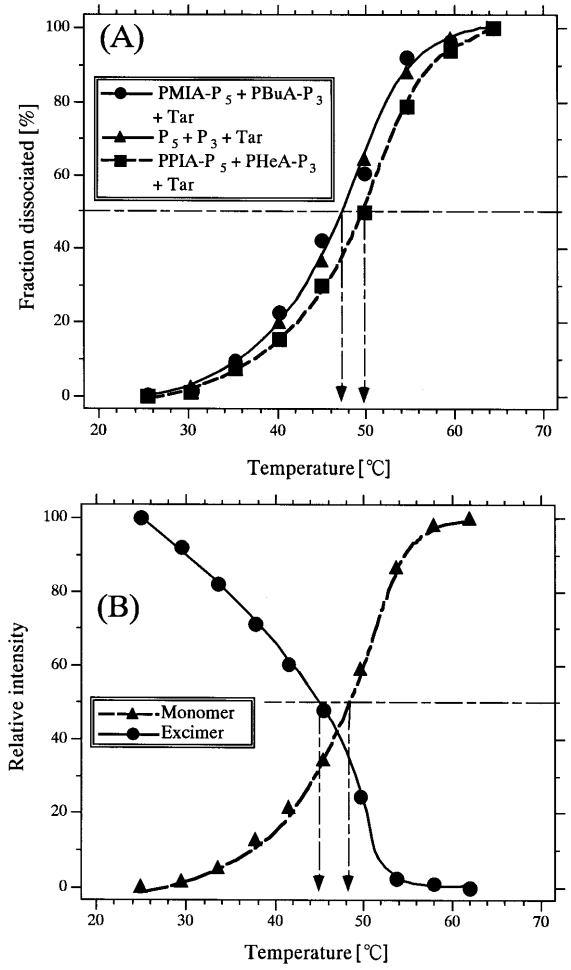

Figure 6. (**A**) Dissociation profiles of three kinds of hybrid, determined by measuring A_{270} as a function of temperature and (**B**) dissociation profiles of the hybrid between PMIA-P_5/PBuA-P_3 and Tar, prepared by measuring excimer and monomer fluorescence intensities at 495 and 378 nm, respectively, as a function of temperature. The concentration of each dye-labeled probe, oligonucleotide and Tar was 400 nM in (A) and 100 nM in (B). Other conditions are those in Figure 3 except for temperature.

stabilize the duplex, resulting in a T_m increase (45), we did this evaluation by measuring the T_m values. Figure 6A shows the hyperchromicity-based melting curves for our hybridization system. The melting curve for the duplex between PMIA-P_5/PBuA-P_3 and Tar was similar to that for the duplex of the unlabeled probes (i.e. P_5/P_3 and Tar). Furthermore, the two duplexes had the same T_m value of 47°C. However, the duplex from PPIA-P_5/PHeA-P_3, which was the third worst probe combination for excimer emission (Fig. 5B), exhibited a more gentle slope of the curve and its T_m value was 50°C.

For further interpretation of duplex formation, we obtained the melting curve for the hybrid between PMIA-P_5/PBuA-P_3 and Tar by monitoring its fluorescence spectrum. By defining the 0 and 100% levels of the duplex as 25 and 62°C, respectively, and the apparent T_m value as that corresponding to the 50% level, the T_m levels (Fig. 6B) were 45 and 48°C for excimer and monomer emissions, respectively. Preliminary experiments indicated that intensities of the monomer emission spectra of both PMIA-P_5 and PBuA-P_3 dissolved in the standard hybridization solution did not change in the 25–65°C range. Therefore, the main reason why monomer emission increased with increasing temperature (Fig. 6B) is the dissociation of pyrene dimers to monomers, accompanied by dissociation from double-stranded to single-stranded oligonucleotides. In fact, the apparent T_m (48°C) for the monomer emission was similar to the T_m (47°C, Fig. 6A) from the hyperchromicity-based measurement. On the other hand, the apparent T_m (45°C) for excimer emission was slightly lower than the T_m (47°C) from the A_{270} measurement and that (48°C) for monomer emission. Generally, excimer emission quantum efficiencies, including that of pyrene, are sensitive to temperature change, decreasing with increasing temperature above room temperature (1,3,31,46). Accordingly, this effect may be additive to the effect of duplex dissociation-based excimer decrease, thereby lowering the apparent T_m more than that expected from hyperchromicity-based measurements. Other (apparent) T_m values were also determined from melting curves (data not shown). In both absorption and fluorescence measurements, there was no appreciable difference between the (apparent) T_m values for the hybrid PMIA-P_5 and Tar (46°C), and that for the hybrid PBuA-P_3 and Tar (48°C). This similarity coincides with the comparison of the predicted free energy changes for these hybridizations (Materials and Methods). In addition, these T_m values were not appreciably different from those for the corresponding hybrids without labels (i.e. P_5 and Tar, and P_3 and Tar).

CD spectra of the hybrids

CD spectra of nucleic acid molecules in solution provide not only reliable information on their overall conformations (47), but also on the interaction responsible for the association of achiral molecules with chiral compounds, such as nucleic acids (48). For the three hybrids PMIA-P_5/PBuA-P_3 and Tar, PPIA-P_5/PHeA-P_3 and Tar, and P_5/P_3 and Tar (2.0 μM each of the probes and Tar), dissolved in the standard hybridization solution, we obtained CD spectra in the wavelength region 260–400 nm. All the spectra exhibited one positive Cotton effect with a peak at ~270 nm. We could not detect any difference among these spectra. Furthermore, we could not detect an induced CD signal at ~340 nm for either the hybrid PMIA-P_5/PBuA-P_3 and Tar, or the hybrid PPIA-P_5/PHeA-P_3 and Tar. These results suggest that pyrene residues do not strongly interact with the helix and/or are not in a chiral environment, despite a slight T_m increase observed for the hybrid PPIA-P_5/PHeA-P_3 and Tar (Fig. 6A).

Interactions of pyrene residues in the duplex

To induce excimer emission, the hybridization conditions, which include the molecular design of the dye-labeled probes, are important not only for pyrene-labeled probes but also for other dye-labeled probes in the future. Studies by Mann *et al.* (18) and Koenig *et al.* (44) involving single-probe hybridization (i.e. not excimer formation) reported that a pyrene conjugated to the terminal of a hybrid through long linker arms intercalates into the duplex or stacks onto a base upon hybridization, resulting in a T_m increase and remarkable fluorescence quenching. In contrast, studies by Kierzek *et al.* (32) and Yamana *et al.* (49) involving single-probe hybridization did not report such a T_m increase and fluorescence quenching. Yamana *et al.* (49) reported that pyrene is conjugated to the 5′-OH and 3′-OH of terminal sugars with the shortest linker arm, -CH_2-, and Kierzek *et al.* (32) reported that a pyrene residue docks into the major groove of a duplex.

However, our hybridizations using PMIA-P_5 and PBuA-P_3, even when they were single-probe hybridizations, showed neither intercalation nor stacking by the criteria of T_m value (Fig. 6) and CD spectrum; this result differs from those reported by Mann *et al*. (18) and Koenig *et al*. (44). However, the differences in length between linker arms of the probes [e.g. 5′-terminal deoxyribose-PO_3^-–$(CH_2)_4$-pyrene] in the studies by Mann *et al*. and Koenig *et al*. and those of our probes (Fig. 2) were too small to explain the discrepancy in the results. Another discrepancy is that our hybridizations showed quenching of monomer fluorescence when one of the probes was not labeled with a pyrene, whereas studies by Kierzek *et al*. (32) and Yamana *et al*. (49) did not. There are two differences in the experimental conditions between our study and all four of those other studies (18,32,44,49): (i) the addition of DMF to hybridization solutions; (ii) in excimer formation, the presence of one pyrene residue close to the other pyrene residue on the hybrid. The DMF addition (>20%) easily recovered the monomer intensity of pyrenes from the quenching observed for single strands (Fig. 4B). For duplexes from the combination of PMIA-P_5 and Tar (without PBuA-P_3), however, the monomer intensity did not easily recover until DMF addition was 40% (Fig. 4B). If the liberation of pyrene residues from an interaction with the duplex (e.g. intercalation) by DMF leads to the formation of an excimer, its enhancement should be observed at a similar concentration. However, such enhancement was observed at a DMF concentration of only ~10% (Fig. 4A). Therefore, the DMF addition alone does not explain the enhancement in excimer emission. The existence of an extra pyrene residue close to the other pyrene residue may enhance dimer formation with the aid of DMF molecules. This means that an optimal configuration of the two pyrene residues for intense excimer emission may be affected by pyrene–pyrene interaction, pyrene–duplex interaction (intercalation/stacking) and solvent conditions (including DMF and NaCl addition) as a whole. The optimal conditions thus attained in this study may restrict a pyrene residue to being intercalated or stacked, thereby enhancing excimer formation.

Detectability of excimer emission

The quantum efficiency of excimer emission of the hybrid between PMIA-P_5/PBuA-P_3 and Tar was 0.056 ± 0.007 (mean ± SD, four measurements using separate preparations of the same probes) under the optimal hybridization conditions determined in this study. The extinction coefficient of a pair of pyrene residues in the duplex was 41.8/mM/cm. When we compare these quantum efficiencies and extinction coefficient values with those of widely used labels for nucleic acid detection, namely the fluorescein family of dyes [e.g. ~0.4 (50) and 67/mM/cm at 490 nm (51) in an aqueous neutral buffer solution], the detectability of pyrene excimer emission is one order of magnitude lower than that of fluorescein fluorescence (assuming that other instrumentation conditions are the same). Therefore, one should use a high sensitivity spectrofluorometer, such as a photon-counting type model, when attempting to detect a low concentration (e.g. <1 nM) of hybrids by the ETPH method.

Determination of 16S rRNA content in a cell of *V.mimicus*

To demonstrate the ETPH method, we analyzed 16S rRNA in an extract from *V.mimicus* with synthetic oligoribonucleotides as a standard to determine 16S rRNA content in a cell of the bacterium. There were prerequisites for the measurements: (i) a high yield of RNA for extract preparation; (ii) a small number of steps in the analysis for accuracy in the assay. The first prerequisite was achieved using the TRI Reagent® extraction protocols in a single step of RNA isolation and two steps of alcohol precipitation, of which the yield of RNA has proven to be extremely high in a wide variety of biological materials (52). The second prerequisite was accomplished using the ETPH method where an aliquot of the extract was mixed with the standard hybridization solution containing 2 mM EDTA in a cuvette.

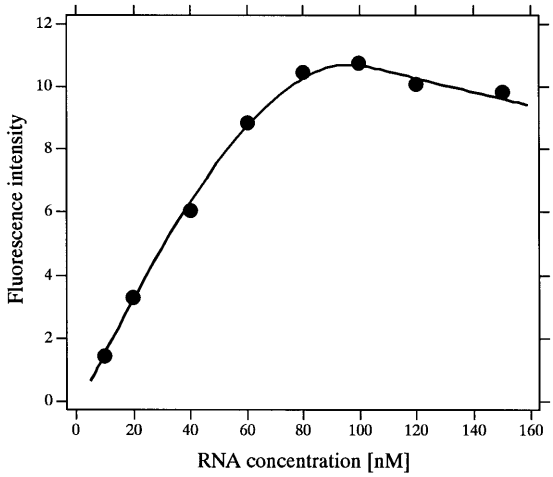

Figure 7. Calibration curve for determining 16S rRNA of *V.mimicus* by the ETPH method. The reaction mixture contained 100 nM each of PMIA-P_5 and PBuA-P_3 and various concentrations of the target 32mer ribonucleotide, whose sequence was the same as that for Tar (U replaces T). Other conditions are those listed in Materials and Methods.

Analytical data normalized to the number of cells was 1.85 ± 0.40 × 10^4 molecules/cell (mean ± SD, four experiments), which is comparable with the data (1.87 × 10^4 molecules/cell) for *Escherichia coli* B/r cells in exponential growth phase (53). A typical example of RNA calibration curves (Fig. 7) shows that at least 10 nM ribonucleotide can be detected using a commercially available spectrofluorometer. This calibration curve had a peak at 100 nM RNA, which is the same concentration as the added probes. This agreement in concentration verifies the practicality of determining the concentrations of pyrene-labeled probes using **1** (Materials and Methods). Furthermore, when the target concentration exceeded 100 nM, the decrease in excimer emission was gradual; even when the target concentration was six times greater (600 nM) than the probe concentration, excimer emission still remained ~1/3 of the maximum intensity. This implies that two types of probe molecules have a strong tendency to hybridize to an identical target molecule; in other words, the target that simultaneously forms two duplexes is more stable than the target that has a duplex on one half and a staggered sequence on the other half.

CONCLUSION

We have been developing a homogeneous nucleic acid hybridization method called the excimer-forming two-probe hybridization (ETPH) method. Using pyrene-labeled probes, we investigated the optimal molecular design of probes and assay conditions for

the ETPH method. Intense excimer emission is attained using a combination of a pyrenemethyliodoacetamide-introduced probe and a pyrenebutanoic acid-introduced probe in an assay mixture containing 20% (v/v) DMF and 0.2 M NaCl at pH 7. The quantum efficiency of this combination was 0.056 ± 0.007. The excimer emission may be variable due to the relative configuration of the two pyrene molecules in a hybrid. We demonstrated the practicality of using the ETPH method for homogenous assays by determining that the content of 16S rRNA in a cell of *Vibrio mimicus* ATCC 33655 is 18 500 molecules/cell on average.

ACKNOWLEDGEMENTS

We thank Dr M. Nishimura (Ocean Researsh Institute, University of Tokyo) for his valuable advice on *Vibrio* detection and Prof. T. Hiratsuka (Department of Chemistry, Asahikawa Medical College) for his guidance on the CDI method. This research was one topic in the National Project for Development of Biosensors in the Food Industry, supported by a grant from the Japanese Ministry of Agriculture, Forestry and Fisheries to Hamamatsu Photonics through the project implementation body, the Society for Techno-Innovation of Agriculture, Forestry and Fisheries.

REFERENCES

1 Birks,J.B. (1970) *Photophysics of Aromatic Molecules*. John Wiley & Sons, London, UK, pp. 301–371.
2 Robertson,J.M. and White,J.G. (1947) *J. Chem. Soc*., 358–368.
3 Birks,J.B., Lumb,M.D. and Munro,I.H. (1964) *Proc. R. Soc. Lond. A*, **280**, 289–297.
4 Kinnunen,P.K.J., Koiv,A. and Mustonen,P. (1993) In Wolfbeis,O.S. (ed.), *Fluorescence Spectroscopy. New Methods and Applications*. Springer-Verlag, Berlin, Germany, pp. 159–171.
5 Van Arman,S.A. and Czarnik,A.W. (1990) *J. Am. Chem. Soc*., **112**, 5376–5377.
6 Zama,M., Bryan,P.N., Harrington,R.E., Olins,A.L. and Olins,D.E. (1978) *Cold Spring Harbor Symp. Quant. Biol*., **42**, 31–41.
7 Morawetz,H. (1979) *Science*, **203**, 405–410.
8 Betcher-Lange,S.L. and Lehrer,S.S. (1978) *J. Biol. Chem*., **253**, 3757–3760.
9 Ueno,A., Suzuki,I. and Osa,T. (1990) *Anal. Chem*., **62**, 2461–2466.
10 Schildkraut,C.L., Marmur,J. and Doty,P. (1961) *J. Mol. Biol*., **3**, 595–617.
11 Tijssen,P. (1993) *Hybridization with Nucleic Acid Probes*. Part I: *Theory and Nucleic Acid Preparation*. Elsevier, Amsterdam, The Netherlands, pp. 1–17.
12 Kricka,L.J. (ed.) (1992) *Nonisotopic DNA Probe Techniques*. Academic Press, San Diego, CA.
13 Meinkoth,J. and Wahl,G. (1984) *Anal. Biochem*., **138**, 267–284.
14 Matthews,J.A. and Kricka,L.J. (1988) *Anal. Biochem*., **169**, 1–25.
15 Cantor,C.R. (1996) *Nature Biotechnol*., **14**, 264.
16 Lee,L.G., Connell,C.R. and Bloch,W. (1993) *Nucleic Acids Res*., **21**, 3761–3766.
17 Ebata,K., Masuko,M., Ohtani,H. and Kashiwasake-Jibu,M. (1995) *Photochem. Photobiol*., **62**, 836–839.
18 Mann,J.S., Shibata,Y. and Meehan,T. (1992) *Bioconjugate Chem*., **3**, 554–558.
19 Hileman,R.E., Parkhurst,K.M., Gupta,N.K. and Parkhurst,L.J. (1994) *Bioconjugate Chem*., **5**, 436–444.
20 Kita-Tsukamoto,K., Oyaizu,H., Nanba,K. and Simidu,U. (1993) *Int. J. Syst. Bacteriol*., **43**, 8–19.
21 Nishimura,M., Kita-Tsukamoto,K., Kogure,K. and Ohwada,K. (1992) *Bull. Jpn. Soc. Microbial Ecol*., **7**, 43–46.
22 Breslauer,K.J., Frank,R., Blöcker,H. and Marky,L.A. (1986) *Proc. Natl Acad. Sci. USA*, **83**, 3746–3750.
23 Czworkowski,J., Odom,O.W. and Hardesty,B. (1991) *Biochemistry*, **30**, 4821–4830.
24 Gottikh,B.P., Krayevsky,A.A., Tarussova,N.B., Purygin,P.P. and Tsilevich,T.L. (1970) *Tetrahedron*, **26**, 4419–4433.
25 Hiratsuka,T. (1997) *Biophys. J*., **72**, 843–849.
26 Fasman,G.D. (1975) *Handbook of Biochemistry and Molecular Biology. Nucleic Acids*, 3rd Edn. CRC Press, Cleveland, OH, Vol. 1, p. 589.
27 Parker,C.A. and Rees,W.T. (1960) *Analyst*, **85**, 587–600.
28 Melhuish,W.H. (1961) *J. Phys. Chem*., **65**, 229–235.
29 Kaper,J., Lockman,H., Colwell,R.R. and Joseph,S.W. (1979) *Appl. Environ. Microbiol*., **37**, 91–103.
30 Sambrook,J., Fritsch,E.F. and Maniatis,T. (1989) *Molecular Cloning: A Laboratory Manual*, 2nd Edn. Cold Spring Harbor Laboratory Press, Cold Spring Harbor, NY, pp. 7.3–7.5.
31 Birks,J.B. (1968) *Acta Phys. Pol*., **34**, 603–617.
32 Kierzek,R., Li,Y., Turner,D.H. and Bevilacqua,P.C. (1993) *J. Am. Chem. Soc*., **115**, 4985–4992.
33 Mohammadi,S., Slama-Schwok,A., Léger,G., Manouni,D.E., Shchyolkina,A., Leroux,Y. and Taillandier,E. (1997) *Biochemistry*, **36**, 14836–14844.
34 McConaughy,B.L., Laird,C.D. and McCarthy,B.J. (1969) *Biochemistry*, **8**, 3289–3295.
35 Schmeckpeper,B.J. and Smith,K.D. (1972) *Biochemistry*, **11**, 1319–1326.
36 Nakajima,A. (1971) *Bull. Chem. Soc. Jpn*, **44**, 3272–3277.
37 Schildkraut,C. and Lifson,S. (1965) *Biopolymers*, **3**, 195–208.
38 Dove,W.F. and Davidson,N. (1962) *J. Mol. Biol*., **5**, 467–478.
39 Studier,F.W. (1969) *J. Mol. Biol*., **41**, 199–209.
40 Wolfe,A., Shimer,G.H.,Jr and Meehan,T. (1987) *Biochemistry*, **26**, 6392–6396.
41 Boyland,E. and Green,B. (1962) *Br. J. Cancer*, **16**, 507–517.
42 Stevens,B. (1962) *Spectrochim. Acta*, **18**, 439–448.
43 Hirayama,F. (1965) *J. Chem. Phys*., **42**, 3163–3171.
44 Koenig,P., Reines,S.A. and Cantor,C.R. (1977) *Biopolymers*, **16**, 2231–2242.
45 Berman,H.M. and Young,P.R. (1981) *Annu. Rev. Biophys. Bioengng*, **10**, 87–114.
46 Förster,T. and Seidel,H.-P. (1965) *Z. Physik. Chem. (N.F.)*, **45**, 58–71.
47 Gray,D.M., Ratliff,R.L. and Vaughan,M.R. (1992) *Methods Enzymol*., **211**, 389–406.
48 Brittain,H.G. (1994) In Purdie,N. and Brittain,H.G. (eds.), *Analytical Applications of Circular Dichroism*. Elesevier, Amsterdam, The Netherlands, pp. 307–341.
49 Yamana,K., Nunota,K., Nakano,H. and Sangen,O. (1994) *Tetrahedron Lett*., **35**, 2555–2558.
50 Eis,P.S. and Millar,D.P. (1993) *Biochemistry*, **32**, 13852–13860.
51 Waggoner,A. (1995) *Methods Enzymol*., **246**, 362–373.
52 Chomczynski,P. (1993) *BioTechniques*, **15**, 532–537.
53 Neidhardt,F.C. (1987) In Neidhardt,F.C., Ingraham,J.L., Low,K.B., Magasanik,B., Schaechter,M. and Umbarger,H.E. (eds.), *Escherichia coli and Salmonella typhimurium. Cellular and Molecular Biology*. American Society for Microbiology, Washington, DC, Vol. 1, pp. 3–6.